



Numerical simulation of perovskite solar cell with porous silicon layer

Badiaa Bachiri*, Khadidja Rahmoun

Unité de Recherche Matériaux et Energies Renouvelables (URMER), University of Tlemcen, Abou Bekr Belkaid, BP 119, 13000, Tlemcen, Algeria, emails: bachiribadi3a@gmail.com (B. Bachiri), k_rahmoun@yahoo.fr (K. Rahmoun)

Received 20 May 2022; Accepted 6 October 2022

ABSTRACT

As one of the most promising photovoltaic technologies, perovskite solar cells have attracted attention with several properties and high efficiency. In this paper, a p-i-n perovskite solar cell with the structure of (PSi/CuO/CH₃NH₃PbI₃/ZnO) was investigated using solar cell capacitance simulator which has achieved a power conversion efficiency of $\eta \sim 8.69\%$. In order to investigate its performance, porous silicon (PSi) was suggested to know its impact on this structure. The results reveal significantly the effect of porous silicon on the performance of solar cell's structure. We studied the influence of thickness and band gap of absorber layer also dopant concentration of PSi layer. The results demonstrated the highest agreement with the experiments.

Keywords: Perovskite solar cell; Porous silicon; Efficiency; Solar cell capacitance simulator

1. Introduction

The research community has been interested by metal halide perovskites in recent years, partly because of a combination of their optoelectronic properties unexpected as sustainable materials used as absorber layers in photovoltaic (PV) devices. Perovskites are materials described by the formula ABX₃, where A is methylammonium (MA), cesium (Cs), or formamidinium (FA); B is Pb or Sn; and X is I, Cl, or Br [1]. Some of the important characteristics of these perovskites include simple preparation, high sun absorption, and low non-radiative carrier recombination rates and significant carrier mobility [2]. One disadvantage of perovskites is that lead has been found in important concentrations in all high-performance perovskite cells, posing toxicity concerns throughout device production, deployment, and disposal [3]. Spin coating, thermal evaporation, chemical vapor deposition, and other manufacturing procedures for perovskite thin films have all been using and choosing for the perovskites fabrication. Kojima et al. [4] published the first perovskite solar cell (PSC) paper. Methylammonium lead iodide (CH₃NH₃PbI₃) and methylammonium lead bromide

(CH₃NH₃PbBr₃) were solid sensitizers used in dye-sensitized solar cells (DSSCs) with liquid electrolyte. These sensitizers had poor power conversion efficiencies of 3.13% and 3.81%, respectively. Unexpectedly, the test cells created by Lee et al. [5] that replaced porous (TiO₂), an electron conductor, with porous (Al₂O₃), an insulator, performed better than those created without (TiO₂). They also saw a significant increase in voltage. Lin et al. [6] has been study optoelectronic properties of CH₃NH₃PbI₃ perovskite planar devices, where they fabricated an optimum device with an efficiency of 16.5% allowing improved modelling and designing. Bush et al. [7] combined an infrared-tuned silicon heterojunction bottom cell with produced cesium formamidinium lead halide perovskite, Schutt et al. [8] increased the PCE to a record 23.6% with 1 cm² perovskite/silicon tandems. Through the development of experimental techniques to clarify the degradation mechanisms at ZnO/MAPbI₃ interfaces, Schutt et al. [8] increased the PCE to a record 21.1%. They significantly improved the stability of the perovskite/ZnO interface by substituting MA with formamidinium (FA) and cesium (Cs), and they discover that stability compares favorably with SnO₂ based devices under high intensity UV irradiation and

* Corresponding author.

85°C thermal stressing [9]. Originally, this was achieved in photovoltaic devices, whose efficiency rose from 21.1% in 2019 to a certified 32.2% in 2021 [10]. In accordance with this, we study the impact of porous silicon on the MAPbI₃ structure using CuO as hole transport layer and ZnO as electron transport layer using solar cell capacitance simulator (SCAPS) to investigate its efficiency.

2. Material and methods

In this study, a solar cell capacitance simulator (SCAPS) is used to numerically predict the electrical characteristics of the perovskite structure for solar cell devices. The Department of Electronic and Informative Systems at the University of Gent created SCAPS, a software platform used for solar simulation research that is acknowledged and standardized throughout the world (ELIS) [11,12]. SCAPS functioning is based on key equations that represent sunlight collection, electron/hole pair creation, transport, and extraction. Overall, SCAPS enables researchers to address a variety of fundamental nanostructured materials and semiconductor physics issues [9,13]. Fig. 1 represent the conventional p-i-n structure for PSCs. Between the HTM and ETM layers, which are both metal oxides that can be processed using an inorganic solution, is a layer of MAPbI₃ perovskite. Al is employed as the cells' back contact. As previously stated, (CuO, p-type) is utilized for HTM. The ETM layer, on the other hand, is made of metal oxides (ZnO, n-type), and p-type porous silicon (p-PSi) was deposited on top of the structure.

In this study, all materials properties, such as band gap, electron affinity, and so on, must be manually given for each layer in SCAPS. These values must be selected with attention and critical way in order to achieve a successful simulation result. These parameters were primarily chosen from published work in referred journals that took into account a similar fabrication environment, under an optimal temperature $T = 300^{\circ}\text{K}$, a PS layer of porosity 91% with a bang gap value of 1.98 eV [14]. Table 1 summarizes the characteristics of the chosen material for each layer.

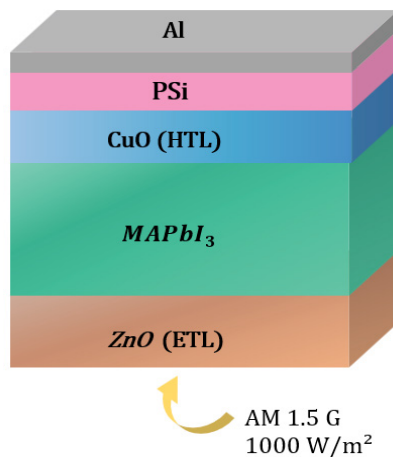


Fig. 1. Layer stack of the simulated perovskite solar cell with MAPbI₃.

It is assumed that the sun's light is AM 1.5G (1,000 W/m²) in all simulations. Auger recombination and radiative band-to-band recombination default generation model are not taken into account. The only recombination mechanism investigated in this study is defect-induced recombination. It is necessary to compare the simulation work to a fabrication structure similar to Fig. 1. In order to demonstrate its validity we compare our results with the work of Kim and Park [19]. Final results are given in Table 2, in which a solar planar PSC is (PSi/CuO/MAPbI₃/ZnO) built and characterized. Bulk defect densities are chosen as the controlling variables to achieve equivalence with the results. For each material, to make the model simple, just one bulk defect grade is evaluated. Bulk defect densities for MAPbI₃ and PSi are evaluated by $1 \times 10^{12} \text{ cm}^{-3}$, $1 \times 10^{15} \text{ cm}^{-3}$ for ZnO and CuO are evaluated by $1 \times 10^{14} \text{ cm}^{-3}$.

3. Results and discussion

Figs. 2 and 3 show the J-V characteristics and QE curves of solar cell-based PSC. Because of the perovskite's increased light absorption, which also shows in the QE rise in the 300–570 nm spectral area, the current density/voltage graph indicated higher current density, also to the higher carrier mobility as well [20,21].

3.1. Impact of MAPbI₃ thickness and PSi on performance of solar cells

To investigate the influence of the absorber's and PSi's thickness. As shown in Fig. 4, the generation of additional

Table 1
Electrical characteristics of several layers

Properties	MAPbI ₃	n-ZnO	CuO	PSi
Thickness (μm)	0.4	0.15	0.149	0.125
E_g (eV)	2.3	3.2	2.17	1.98
χ (eV)	3.93	3.9	3.2	4.09
ϵ_r	10	9.00	7.110	2
N_c (1/cm ³)	2.2×10^{19}	1.21×10^{21}	2.02×10^{17}	2.820×10^{19}
N_v (1/cm ³)	1.8×10^{19}	2×10^{20}	1.1×10^{19}	1.04×10^{19}
N_A (1/cm ³)	00	00	1×10^{18}	1×10^{16}
N_D (1/cm ³)	00	2×10^{19}	00	00
μ_n (cm ² /Vs)	1.1×10^7	2×10^1	2×10^2	1.5×10^3
μ_p (cm ² /Vs)	1.01	1.10^1	8.10^1	4.5×10^2
References	[15]	[16]	[17]	[18]

Table 2
Comparison of the experimental work with the results of the simulation [20]

Structure	J_{sc} (mA/cm ²)	V_{oc} (V)	FF%	$\eta\%$
(PSi/CuO/CH ₃ NH ₃ PbI ₃ /ZnO)	7.8386	1.4195	78.09	8.69
Experimental work [20]	0.41	0.242	41.4	8.21

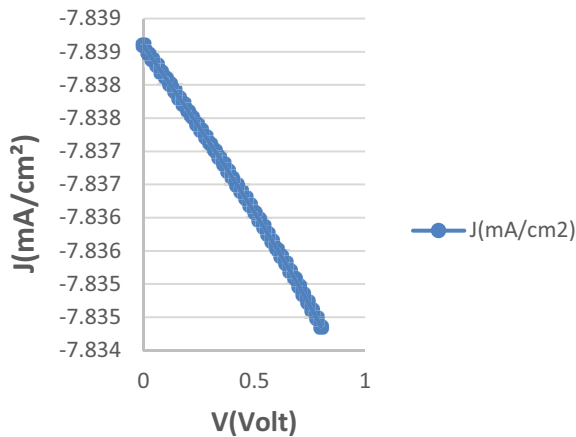


Fig. 2. I-V curve of perovskites solar cell.

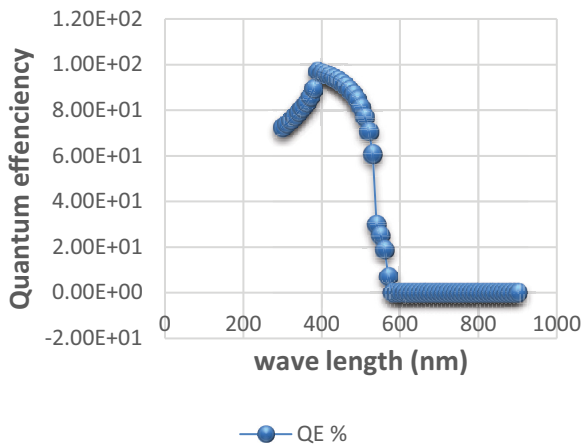


Fig. 3. Variation of quantum efficiency with wavelength.

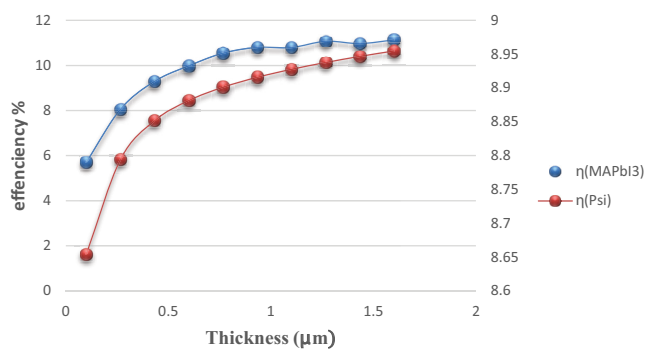


Fig. 4. Effect of MAPbI₃ and PSi thickness on efficiency.

electron-hole pairs in the perovskite, which results an improvement in efficiency, causes power conversion efficiency to grow with increasing thickness. Furthermore, PSi's efficiency increase as the thickness of PSi layer increase because PSi layer absorber the possible long wavelength photons, while for thinner layers the generation takes place near the interfaces [22,23]. The optimum thickness correlate to Kawter et al. work is about 0.125 µm.

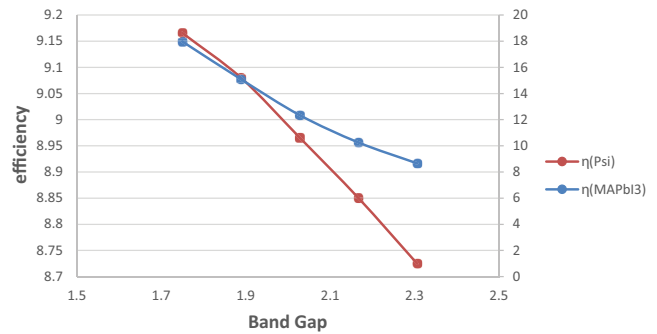


Fig. 5. Effect of MAPbI₃ and PSi band gap on efficiency.

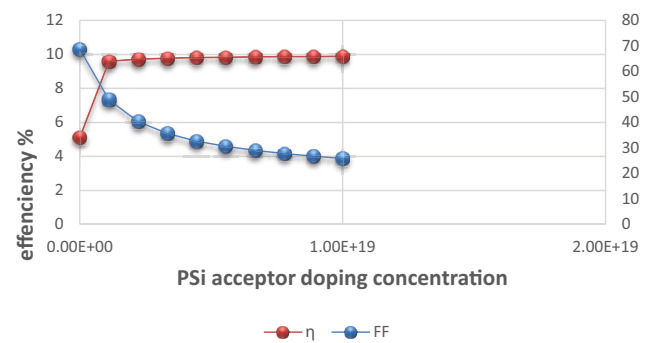


Fig. 6. Effect of PSi acceptor doping concentration on efficiency and fill factor.

3.2. Influence of variation band gap on solar cell performance

Another critical factor that has a substantial impact on device performance is variation in band gap. Fig. 5 represents variation of band gap range in function of efficiency, given from 1.75 to 2.3 eV. As can be seen, efficiency of the perovskite and PSi decrease where the band gap increase, while there is high absorber portion of the wavelength from the MAPbI₃, help the cell to be more stable [24,25]. In addition, it can be observed from the same graph efficiency decrease when band gap of PSi layer increase, because of the rise of refractive index. More porosity increase, refractive index decrease and thereby efficiency increase as well [13,26].

3.3. Effect of doping concentration

To increase the efficiency of the solar cell, doping is one of the most crucial production processes. The simulation was done by changing it from 1.10⁸ to 1.10¹⁹ atom/cm³. As it is shown in Fig. 6, More PSi layer acceptor doping increase, more efficiency increase. It became quite stable from 5.56 × 10¹⁸ atom/cm³ where saturation was taken place. On the other hand, fill factor (FF) is inversely proportional to PSi acceptor doping concentration [27]. Because of that, it noted that a calibrated mix of solar cell materials would be ideal for energy absorption. With the perovskite as an active layer, it can collect the short wavelength photons while the bottom silicon layer absorbs long wavelength photons.

4. Conclusion

In this work, a normal p-i-n planar PSC structure having the configuration of (PSi/CuO/CH₃NH₃PbI₃/ZnO) is performed using the SCAPS-1D simulation software. These results demonstrated that the application of PSi to the cell's surface offers significant promise for PV performance, particularly when thickness and PSi doping concentration are increased. More than 17% of efficiency achieved by this structure where it is improved by changing thickness and doping concentration. Thus, our model was validated with similar experimental work. Consequently, our simulation-based study offers valuable insights on this typical porous silicon and its impact on the perovskites as efficient absorber layer.

References

- [1] Y. Raoui, H. Ez-Zahraouy, N. Tahiri, O. El Bounagui, S. Ahmad, S. Kazim, Performance analysis of MAPbI₃ based perovskite solar cells employing diverse charge selective contacts: simulation study, *Sol. Energy*, 193 (2019) 948–955.
- [2] M.A. Green, A. Ho-Baillie, H.J. Snaith, The emergence of perovskite solar cells, *Nat. Photonics*, 8 (2014) 506–514.
- [3] M.M. Tavakoli, M. Saliba, P. Yadav, P. Holzhey, A. Hagfeldt, S.M. Zakeeruddin, M. Grätzel, Synergistic crystal and interface engineering for efficient and stable perovskite photovoltaics, *Adv. Energy Mater.*, 9 (2019) 1802646, doi: 10.1002/aenm.201802646.
- [4] A. Kojima, K. Teshima, Y. Shirai, T. Miyasaka, Organometal halide perovskites as visible-light sensitizers for photovoltaic cells, *J. Am. Chem. Soc.*, 131 (2009) 6050–6051.
- [5] M.M. Lee, J. Teuscher, T. Miyasaka, T.N. Murakami, H.J. Snaith, Efficient hybrid solar cells based on meso-superstructured organometal halide perovskites, *Science*, 338 (2012) 643–647.
- [6] Q. Lin, A. Armin, R.C.R. Nagiri, P.L. Burn, P. Meredith, Electro-optics of perovskite solar cells, *Nat. Photonics*, 9 (2015) 106–112.
- [7] K.A. Bush, A.F. Palmstrom, J.Y. Zhengshan, M. Boccard, R. Cheacharoen, J.P. Mailoa, D.P. McMeekin, R.L.Z. Hoye, C.D. Bailie, T. Leijtens, I.M. Peters, M.C. Minichetti, N. Rolston, R. Prasanna, S. Sofia, D. Harwood, W. Ma, F. Moghadam, H.J. Snaith, T. Buonassisi, Z.C. Holman, S.F. Bent, M.D. McGehee, 23.6%-efficient monolithic perovskite/silicon tandem solar cells with improved stability, *Nat. Energy*, 2 (2017) 17009, doi: 10.1038/nenergy.2017.9.
- [8] K. Schutt, P.K. Nayak, A.J. Ramadan, B. Wenger, Y.-H. Lin, H.J. Snaith, Overcoming zinc oxide interface instability with a methylammonium-free perovskite for high-performance solar cells, *Adv. Funct. Mater.*, Special Issue: Emerging Photovoltaic Materials and Devices, 29 (2019) 1900466, doi: 10.1002/adfm.201900466.
- [9] S. Sarker, M.T. Islam, A. Rauf, H.A. Jame, M.R. Jani, S. Ahsan, M.S. Islam, S.S. Nishat, K.M. Shorowordi, S. Ahmed, A SCAPS simulation investigation of non-toxic MAgel₃-on-Si tandem solar device utilizing monolithically integrated (2-T) and mechanically stacked (4-T) configurations, *Sol. Energy*, 225 (2021) 471–485.
- [10] M. Burgelman, P. Nollet, S. Degraeve, Modelling polycrystalline semiconductor solar cells, *Thin Solid Films*, 361–362 (2000) 527–532.
- [11] J. Verschraegen, M. Burgelman, Numerical modeling of intra-band tunneling for heterojunction solar cells in SCAPS, *Thin Solid Films*, 515 (2007) 6276–6279.
- [12] M. Burgelman, K. Decock, A. Niemegeers, J. Verschraegen, S. Degraeve, SCAPS Manual Most Recent, University of Gent, Belgium, 2021.
- [13] K. Rahmoun, S. Fakiri, Modeling to predict effective dielectric constant of porous silicon low-dielectric-constant thin films, *Spectrosc. Lett., An Int. J. Rapid Commun., Special Issue: Fourth International Meeting on Dielectric Materials (IMDM'4)* Marrakech, Morocco, 47 (2014) 348–355.
- [14] J. Laali, A. Hamedani, Gh. Alahyarizadeh, A. Minucheher, Performance analysis of the perovskite solar cells by a realistic, DFT-accurate optical absorption spectrum, *Superlattices Microstruct.*, 143 (2020) 106551, doi: 10.1016/j.spmi.2020.106551.
- [15] K.D. Jayan, V. Sebastian, J. Kurian, Simulation and optimization studies on CsPbI₃ based inorganic perovskite solar cells, *Sol. Energy*, 221 (2021) 99–108.
- [16] K.D. Jayan, V. Sebastian, Comprehensive device modelling and performance analysis of MASnI₃ based perovskite solar cells with diverse ETM, HTM and back metal contacts, *Sol. Energy*, 217 (2021) 40–48.
- [17] I.A. Habbouche, Etude des Caractéristiques du Silicium Poreux pour Application aux Cellules Photovoltaïques, Master's Degree Thesis, Abou Baker Blkaid University, Tlemcen, 2016.
- [18] K.A. Khalaph, Z.J. Shanan, F. Mustafa Al-Attar, A.N. Abd, A. Mashot Jafar, Fabrication and investigation of hybrid perovskite solar cells based on porous silicon, *Mater. Today: Proc.*, 20 (2019) 605–610.
- [19] Y. Kim, B. Park, Understanding charge trapping/detrapping at the zinc oxide (ZnO)/MAPbI₃ perovskite interface in the dark and under illumination using a ZnO/perovskite/ZnO test platform, *Nanoscale*, 10 (2018) 20377–20383.
- [20] A. Shaker, M. ElSabbagh, M.M. El-Banna, Impact of nonuniform gate oxide shape on TFET performance: a reliability issue, *Physica E*, 106 (2019) 346–351.
- [21] K.A. Salman, K. Omar, Z. Hassan, Effective conversion efficiency enhancement of solar cell using ZnO/PS antireflection coating layers, *Sol. Energy*, 86 (2012) 541–547.
- [22] R.C. Anderson, R.S. Muller, C.W. Tobias, Investigations of the electrical properties of porous silicon, *The Electrochem. Soc.*, 138 (1991) 3406–3411.
- [23] A. Amat, E. Mosconi, E. Ronca, C. Quarti, P. Umari, M.K. Nazeeruddin, M. Grätzel, F.D. Angelis, Cation-induced band-gap tuning in organohalide perovskites: interplay of spin-orbit coupling and octahedra tilting, *Nano Lett.*, 14 (2014) 3608–3616.
- [24] X. Ke, J. Yan, A. Zhang, B. Zhang, Y. Chen, Optical band gap transition from direct to indirect induced by organic content of CH₃NH₃PbI₃ perovskite films, *Appl. Phys. Lett.*, 107 (2015) 091904, doi: 10.1063/1.4930070.
- [25] S. Jiang, Y. Fang, R. Li, H. Xiao, J. Crowley, C. Wang, T.J. White, W.A. Goddard, Z. Wang, T. Baikie, J. Fang, Pressure-dependent polymorphism and band-gap tuning of methylammonium lead iodide perovskite, *Angew. Chem. Int. Ed.*, 128 (2016) 6650–6654.
- [26] K.A. Salman, K. Omar, Z. Hassan, The effect of etching time of porous silicon on solar cell performance, *Superlattices Microstruct.*, 50 (2011) 647–658.
- [27] J. Laali, A. Hamedani, Gh. Alahyarizadeh, A. Minucheher, Performance analysis of the perovskite solar cells by a realistic, DFT-accurate optical absorption spectrum, *Superlattices Microstruct.*, 143 (2020) 106551, doi: 10.1016/j.spmi.2020.106551.